Sulfur contaminations inhibit depolymerization of Kraft lignin

Dideolu Daniel, Lavrent Khachatryan, Carlos Astete, Rubik Asatryan, Cosmin Marculescu, Dorin Boldor

PII: S2589-014X(19)30231-2

DOI: https://doi.org/10.1016/j.biteb.2019.100341

Reference: BITEB 100341

To appear in: *Bioresource Technology Reports*

Received date: 24 October 2019

Accepted date: 26 October 2019

Please cite this article as: D. Daniel, L. Khachatryan, C. Astete, et al., Sulfur contaminations inhibit depolymerization of Kraft lignin, *Bioresource Technology Reports*(2019), https://doi.org/10.1016/j.biteb.2019.100341

Sulfur Contaminations Inhibit Depolymerization of Kraft Lignin

Dideolu Daniel [a], Lavrent Khachatryan [b]*[1], Carlos Astete [a], Rubik Asatryan [c], Cosmin Marculescu [d], Dorin Boldor [a]*[2]

[a] Department of Biological & Agricultural Engineering, Louisiana State University (LSU) and LSU AgCenter, Baton Rouge, Louisiana 70803, USA
[b] Department of Chemistry, Louisiana State University, Baton Rouge, Louisiana 70803, USA
[c] Department of Chemical and Biological Engineering, University at Buffalo, The State University of New York, Buffalo, New York, 14226, United States
[d] Faculty of Power Engineering, University Politehnica of Bucharest, Bucharest 060042, Romania

* Correspondence:
Lavrent Khachatryan: lkhach1@lsu.edu ; Tel.: +1-225-578-4417
Dorin Boldor: dboldor@agcenter.lsu.edu; Tel.: +1-225-578-7762

Declaration of interest: none.

---

[1] Corresponding author
[2] Corresponding author

ABSTRACT

Softwood Kraft lignin (s-KL) and methanol-fractionated extracted Kraft lignin (ex-KL) samples were thermally depolymerized via fractional (step-wise) pyrolysis at temperatures from 175°C to 700°C in an isothermal System for Thermal Diagnostic Studies (STDS) reactor. Major pyrolysis products include guaiacols, vanillins, phenols, syringols, and sulfur-containing compounds. Sulfur-containing compounds, as intrinsic contaminants (both adsorbed and covalently bound to KL matrixes), strongly inhibited the formation of pyrolysis products. The lesser the sulfur content in the KL matrix, the higher the yields of major pyrolysis products. The high yields and early release of tar components from pyrolysis of ex-KL were attributed to the initial pretreatment of s-KL (Soxhlet extraction in methanol) causing a decrease in sulfur content from 3.61% (s-KL) to 2.91% (ex-KL). Mechanistic explanations for the absence of sulfur-containing bio-oil products, inhibitory effect of sulfur-containing compounds, and the relatively high char content in depolymerization of both lignin substrates, are developed.

KEYWORDS: Kraft lignin; sulfur; pyrolysis; fractional; bio-oil

1. INTRODUCTION

The need to harness lignocellulosic biomass to produce cost-competitive renewable fuels has become increasingly critical over the past decade due to rising global energy demands and the need to bolster energy security across nations. Pyrolysis, the rapid thermochemical decomposition process that can be used to convert biomass into liquid fuels, synthesis gas and chemicals in the absence of oxygen, has been used to investigate the chemical structure and product distribution of several lignin-derived biomass. Softwood Kraft Lignin (s-KL), a type of technical lignin, is a promising feedstock with potential applications in a variety of large-scale industrial operations that emphasize green chemical and sustainable material production (Brodin et al., 2009).

The presence of sulfur-based compounds in the lignin derived via the Kraft process is significant due to the use of sulfuric acid as an acidifying agent for black liquor (Vishtal & Kraslawski, 2011). Investigative studies focusing on the effect of co-existing impurities in Kraft lignin such as sulfur-containing species in form of free sulfur, sulfides, sulfites, sulfones, sulfates, disulfides, polysulfides, thiols, etc. on pyrolysis process of KL are scarce or inconclusive (Evdokimov et al., 2018). The nature of the sulfur groups has been well described in a number of publications , thus leading to the general belief that sulfur is present in lignin mostly as organically bound sulfur, sulfate ions, elemental sulfur, and adsorbed polysulfide forms (Svensson, 2008). About half the amount of bound sulfur has been shown to be in form of disulfide, R_2S_2 (oxidized mercaptan groups) and the other half was attached to the carbon atom(s) (thiirane structures – sulfur attached to two carbon atoms) (Evdokimov et al., 2018).

The relative distribution of the sulfur content in the studied softwood lignin was reported as follows (Svensson, 2008): ~ 29% as inorganic sulfur, ~1% as elemental sulfur, and ~70% as organically bound sulfur. Additionally, MeSH as well as $(Me)_2S$ are released as by-products of "kraft pulping" in pulp mills and remain as residue in black liquor (Kouisni et al., 2016).

Nevertheless, not much attention has been paid to the effect of sulfur-based intrinsic impurities (Evdokimov et al., 2018; Han et al., 2018) on KL pyrolysis, even though the pyrolysis of softwood KL dates back to the early 1970s (McCarthy & Islam, 1999). Caballero *et al.* (Caballero et al., 1997) studied the primary reactions from the pyrolysis of powdered Kraft lignin (1.7 % sulfur content) in a Pyroprobe-1000 tubular secondary reactor set-up at 450 ^{o}C – 900 ^{o}C. Results showed that decomposition of lignin occurs at a wider temperature range than those of cellulose and hemicelluloses, and that lignin products obtained at lower temperatures are those likely to come from side groups of the complex 3D aromatic lignin polymer. However, products obtained by Caballero *et al.* (Caballero et al., 1997) differ substantially from those reported lately by Brodin *et al.* (Brodin et al., 2010). Sudden occurrence of products was noticed throughout the entire 200 ^{o}C – 900 ^{o}C interval in their study of the stepwise analytical pyrolysis of pure pine/sprice softwood Kraft lignin, although most products were formed at the 500 ^{o}C – 600 ^{o}C range and none were detected beyond 700^{o}C.

Nowakowski *et al.* (Nowakowski et al., 2010) compared the results from fast pyrolysis of different lignin types (sulfur-free and sulfur-containing) from several international studies. The highly-purified ALM (Asian Lignin Manufacturing Ltd.) lignin exhibited a much wider range of decomposition compared to the non-high-purity ETEK lignin (SEKAB E-Technology Corp., Sweden) from TGA and DTA analyses.

The pyrolysis of the sulfur-free lignin in a micro-oven pyrolyzer-GC/MS yielded higher guaiacols, phenols, other degradation products, and hydrocarbons compared to the sulfur-containing lignin. Nowakowski et al. (Nowakowski et al., 2010) found that the excessive cellulose as impurities also had similar effects of reducing bio-oil yield while making it hard for the lignin to be processed in the fast pyrolysis reactors.

Therefore, the sulfur content in KL hampers its industrial potential due to release of sulfur-containing gas phase compounds into environment and the reduced yields of bio-oil during pyrolysis. Moreover, lack of sulfur in bio-oil components (phenolics, guaiacols, syringols etc.) is intriguing, and this work attempts to provide an original approach to understanding this phenomenon. This manuscript describes an initial series of studies to illustrate the effects of sulfur containing contaminants (free and/or bound) on the depolymerization of KL, particularly, on the yield of bio-oil generation. Our current research represents in detail the fractional (step-wise) pyrolysis of non-treated, softwood Kraft lignin (s-KL) versus treated (i.e. extracted by methanol) Kraft lignin (ex-KL) in the temperature range of 175 ^{o}C – 700 ^{o}C; the sensitivity of the yields of produced total tar as a function of released sulfur compounds from pyrolysis of both, s-KL and ex-KL is demonstrated. A mechanistic explanation of the role of sulfur contaminants on product distribution as well as char formation is presented for the first time to our knowledge.

2. MATERIALS AND METHODS

2.1. Materials and Methods

The s-KL alkaline lignin (pH = 9.0) was supplied from TCI America (Portland, OR) as a black powder. The particle size of the alkaline lignin used was < 125 μm. The sulfate content as an ignition residue was 23.6%, methoxyl group content – 11.9%, and water – 5.5% (Certificate of Analysis). The s-KL was employed for pyrolysis experiments as received. A fraction derived by Soxhlet extraction of s-KL by methanol (KL solubility in methanol ~ 6.1g/kg (Melro et al., 2018)) was used to obtain the hydrophobic portion (Norgren & Edlund, 2001) referred to here as the extracted KL (ex-KL).

For the determination of sulfur content in the lignin samples, wet digestion followed by inductively coupled plasma (ICP) analysis was used. The s-KL and ex-KL used contained 3.61% (w) and 2.91% (w) sulfur respectively, as determined by ICP-MS analysis.

The structural characteristics of both initial and pyrolyzed (in form of char) softwood and extracted Kraft lignins were examined by taking FT-IR spectra recorded from 4000 cm^{-1} to 400 cm^{-1} at a resolution of 4 cm^{-1} in reflectance mode using the Bruker Tensor 27 FT-IR Spectrometer (Bruker Optics, Billerica, MA) and using the OPUS 7.2 Data Collection program for data processing.

XPS analysis of initial and pyrolyzed biomass samples was performed on an ESCA 2SR X-ray Photoelectron Spectroscope (Scienta Omicron, Denver, CO, USA) equipped with mono-chromated Al Kα X-ray source (15 kV, 450 W, vacuum $< 4.6 \times 10^{-9}$ mbar) to determine the quantitative elemental compositions and the bonding states of atoms in the biomass samples. Survey and high-resolution scans of individual elements were recorded and binding energies for the high-resolution spectra were calibrated by setting C-C peak at 284.8 eV in post-data processing using Casa XPS processing software.

2.1.1. Preparation of extracted Kraft lignin (ex-KL)

The ex-KL was prepared in the following manner: about 30 g of KL was placed in a Soxhlet extraction thimble unit connected to a round bottom flask containing 100 ml of methanol (technical grade, Thermo Fisher Scientific, Morris, NJ). The alkaline lignin was extracted for over 24 h to obtain the hydrophobic alkaline lignin fraction, after which the solvent was evaporated from the sample with a Rotavapor R-100 rotary evaporator (Buchi Corp., New Castle, DE). The solid product was first air dried, and then further dried under high vacuum at 40

°C for 48 h. In all, about 3 g highly hydrophobic lignin was extracted and was kept in a desiccator for experiments. The particle size of the extracted Kraft lignin was < 150 µm.

2.1.2. Fractional pyrolysis procedure

The fractional pyrolysis of a biomass sample is a protocol that involves a continuous pyrolysis of the sample, i.e. the same sample is continually heated at each pyrolysis temperature, until no significant products are formed (Bennadji et al., 2018).

2.2. Experimental setup

The decomposition peculiarities of softwood and modified Kraft lignins were performed in a system for thermal diagnostic studies (STDS) reactor (Bennadji et al., 2018) (Figure 1). The STDS consists of the reactor compartment, the temperature control console, sample injection port, a cryogenic trap, and a detection system comprising of a GC–MS. The STDS, via its in-line system, allows the quantitative transport of organic materials from a reactor furnace through a transfer line at 280 ^{o}C to a GC injection port where products are cryogenically trapped at -60 ˚C. The STDS with modified reaction chamber consists of a vertical movable sample holder with a basket at the end, a quartz pyrolysis reactor (7 mm ID x 110 mm long) and a 30 mm-central section located in the isothermal zone of the furnace.

The lignin sample in the deactivated quartz basket (o.d.= 4 mm, length = 8mm, sample mass ~ 8mg at thickness of 2-3 mm) was purged by ultra-high purity N_2 gas for 3 minutes at room temperature in a cold zone, outside of the heated section of the reactor. The basket was then inserted rapidly into the isothermal zone of the preheated reactor at specified temperature to be pyrolysed for 3 minutes. A typical gas residence time of 0.2 s was maintained via flow rate adjustment to reduce homogeneous gas-phase reactions, aid rapid removal of reaction products and ensure uniformity between temperature runs. The pyrolysis gas flow was varied such that the residence time was held constant for every temperature change. Three thermocouples were placed at three locations of the quartz tubular reactor to measure established temperatures during pyrolysis. After each run, the same solid lignin residue was moved back to the cold zone for 3 min, cooled to room temperature by flow of N_2 gas in readiness for pyrolysis at the next temperature, starting at 175 ºC in 25 °C (or 50 ^{o}C at higher temperatures) increments until a final temperature at which product formation is negligible. Upon the completion of each pyrolysis run, the mass loss by weight was determined with an analytical balance (accuracy of ± 10^{-4} mg).

2.3. Characterization of lignin samples and pyrolysis products by GC-MS

The mass (or peak area) percentage yields, retention times, and other peak properties of evolved organic volatiles were determined by GC-MS analysis. The pyrolysis products from the injection port passed into an in-line GC-MS system (Agilent 6890N gas chromatograph equipped with a 5973N mass selective detector-MSD). The pyrolysis volatile products initially were trapped and condensed with cryogenic nitrogen (-60 ^{o}C) at the head of capillary column (Agilent J&W DB-5*ms* Ultra Inert GC Column, 30 m x 0.25 mm x 0.25 μm). After each pyrolysis experiment products were resolved by chromatographic separation using the following temperature program: from -60 ºC to 180 ºC at 4 ºC /min and 1 min hold time at 180 ^{o}C, and then ramped at 10 ºC /min to a final temperature of 300 ºC and held for 5 min. The mass spectra were operated in EI mode at 70 eV and scanned from 10 to 650 m/z at 2.5 scans/s frequency.

The progress of data acquisition and product analysis was monitored using Mass Hunter Workstation software (version B.07.02). The chromatographic peaks were identified based on Wiley and NIST 2005 mass spectral libraries alongside retention times of standard mixtures. All reactions were performed at least in duplicates (commonly in triplicates) and average product yields were determined. The experimental reproducibility was within 2-5 % variation for the mass loss profiles and yields of lignin volatiles. Characteristic GC-MS chromatograms from s- and ex-KLs pyrolysis are presented in the e-supplementary data of this work.

3. RESULTS AND DISCUSSION

3.1. Profiles of mass loss for s-KL and ex-KL

Fractional pyrolysis of two Kraft lignins was carried out in a vertical semi-batch reactor with residence time of 0.2 s at temperatures from 175 ^{o}C to 700 ^{o}C as described above. The pattern of weight losses for lignins are depicted in Figure 2, alongside the first derivative of weight loss of the lignins vs. temperature (dW'/dt). On the derivative curves, the positions of the peaks show the temperatures at which maximum rate of weight loss occurred. The peaks (shown by a noticeable change in slope of the thermal decomposition profiles) can be seen at 200 ^{o}C and 300 ^{o}C for s-KL and 175 ^{o}C and 325 ^{o}C for ex-KL biomass.

It is common for lignin samples to have initial decrease in weight due to water removal (Brebu et al., 2011; Yang et al., 2007) starting at lower temperatures. Smooth mass loss of s-KL was observed until 300 ^{o}C, while an accelerated degradation was detected from 300 to 350 ^{o}C with maximal rate at ~ 300 (310) ^{o}C (Figure 2). No appreciable changes in the rates of lignin degradation were noticed at temperatures beyond 425^{o}C for s-KL. The pattern for ex-KL pyrolysis generally follows the same trend as for s-KL, however, the pyrolysis starts at lower temperature with a high rate, followed by a smoother region from 225 to 300 ^{o}C and with maximal rate at ~ 325(335) ^{o}C, Figure 2. Beyond 425 ^{o}C, both lignins (s-KL and ex-KL) pyrolysis ends up at high content of the char residue namely 47 % for ex-KL and 40% for s-KL at pyrolysis temperature 700 ^{o}C

3.2. Temperature dependence of the yields of volatiles from pyrolysis of s-KL and ex-KL

The pyrolysis of Kraft lignin yields three major groups of products: a residue (char), volatile products (tar) and gases (water, CO, CO_2 and other light gases, including sulfur-based compounds). A characteristic GC-MS track for tar volatiles is represented in the e-supplementary data of this work. The yields of major grouped products detected from pyrolysis of s-KL in descending order of GC-MS peak area percentages, for instance at 300 ^{o}C, were; guaiacol (30.69 %), vanillin (10.63 %), acids & aldehydes (4.97 %), phenolics (1.59 %), and syringols (1.26 %). High content of total sulfur-containing compounds (50.86 %) in gaseous form such as dimethyl sulfide $(CH_3)_2S$, dimethyl disulfide (CH_3SSCH_3), methane thiol (CH_3SH), and sulfur dioxide SO_2 was detected. The molecular structures and formulas of all detected tar compounds are summarized in the e-supplementary data of this work. A representative temperature-distribution of the quantified yields of the major product i.e. guaiacol and its derivatives is presented in Figure 3. The evolution of guaiacols in s-KL pyrolysis started between 225-250°C, reaching its highest peak at 300 ^{o}C and steadily decreased to negligible yields thereafter. A shift of the yields of guaiacol products toward low temperatures and dramatic increase in the yields of guaiacols at 250 °C was observed from pyrolysis of ex-KL, Figure 3a; the evolution of guaiacols started at ~ 200 °C, reached its maximum peak at 250 °C, and steadily declined to negligible amounts beyond 350 °C.

It is currently unclear the cause for the drastic change in the yields of guaiacol and its derivatives at such low temperatures far from the maximal rate of decomposition at ~ 325 ^{o}C from pyrolysis of ex-KL (Figure 2). Detection of the high yields of the major product – guaiacol at low temperatures was also reported in literature from pyrolysis of technical softwood Kraft lignin (Brodin et al., 2010). One likely cause of this trend could be that some guaiacol fractions may have intrinsic character as part of Kraft lignin manufacturing. In fact, Soxhlet extraction of s-KL with methanol to yield ex-KL leads to the release of guaiacol, given that it has been initially captured in the lattice of the Kraft lignin. Some other important products, vanillin and syringols also show similar behaviors during pyrolysis of ex-KL. For instance, the high yields of vanillin were already detected at 250 °C. The yields of phenolics were far less significant for extracted lignin with only a minor peak at 315 °C (not shown).

A summary of the yields of total tar components (total of guaiacols, vanillin, phenolics, and syringols) from fractional pyrolysis of the two lignin substrates (solid lines), and the cumulative yields of the total tar (dashed lines) are provided in Figure 3b. The early release of the major tar components from pyrolysis of fractionated ex-KL (brown lines) corresponds to the early pyrolysis profile of the ex-KL, Figure 2. The yields of total tar from s-KL pyrolysis (~7.2 %, w) are much less than the total tar from ex-KL samples (~ 25%, w) (Figure 3b), thus buttressing the significant observation of a late release of tar components from s-KL pyrolysis (blue solid and dashed lines, Figure 3b) in comparison with the analogous data from ex-KL pyrolysis. It is intriguing whether early detection of tar components and their high yields from pyrolysis of ex-KL depends on the behavior of sulfur-containing compounds detected experimentally or the pretreatment of s-KL makes a significant difference.

3.3 Temperature dependence of the yields of sulfur-containing compounds from pyrolysis of s-KL and ex-KL.

The early release of sulfur-containing compounds (dimethyl sulfide $(CH_3)_2S$, dimethyl disulfide CH_3SSCH_3, methane thiol CH_3SH, sulfur dioxide SO_2) was pronounced in the ex-KL pyrolysis more than for the s- KL (Figure 4a). For extracted fraction of Kraft lignin, a consistent increase in yields of sulfur-compounds was noticed starting from 175 °C up till the maximum peak at 345 °C followed by a steady decline. For s-KL the yields of sulfur-containing compounds were considerable lesser with noticeable yield starting at 300 °C, then a maximum peak at 315 °C, and a steady decline afterwards. The maximum rate of depolymerization of s-KL (Figure 2) reaches at ~ 300(310) °C which matches with the maximum amounts of total sulfur-containing compounds released between ~ 300-315 °C into gas phase. No significant sulfur compounds were detected for pyrolysis temperatures above 400°C. Similarly, the maximum amounts of sulfur-containing compounds in the gas phase released from 315 to 345 °C (Figure 4b) matches with the maximum rate of pyrolysis of ex-KL at ~ 325 °C (Figure 2). In fact, as the yields of released sulfur-containing compounds reach a maximum in the gas phase (Figure 4b) the trend of pyrolysis rate also accelerated for both lignins. Dramatically different behavior was observed in accumulation of tar compounds from both lignins' pyrolysis. Indeed, the decomposition of ex-KL pyrolysis between 175 °C and 250 °C occurred via the release of large amounts of guaiacol (Figure 3a) and vanillin in comparison with the analogous data from s-KL pyrolysis.

The early detection of tar compounds from pyrolysis of ex-KL is likely dependent on the early release of sulfur compounds in the temperature region 175-275 °C, Figure 4b. An alternative explanation could be also the fact that the long-term treatment of the s-KL by methanol (overnight Soxhlet extraction) disturbed the structural properties of s-KL in a way that the ex-KL fraction was more prone to depolymerization at low temperatures, (Figures 2 and 3b). This phenomenon (initial pretreatment) is not without precedent in literature, for instance the initial treatment of lignin increases bio-oil yields via pre-torrefaction (Waters et al., 2017), hydrothermal treatment in subcritical water (Islam et al., 2018), formic acid (Løhre et al., 2017), and ultrasound pretreatment (Karnjanakom et al., 2015). To validate this hypothesis, FTIR analyses of both s-KL and ex-KL samples have been performed along with corresponding residue (char) examination (Figure 5).

The frequencies and nature of the bands of the functional groups of the Kraft lignins are presented in the e-supplementary data of this work. The initial s- and ex- Kraft lignins showed more complex spectra compared to those of the pyrolyzed samples. The absorption band observed at 3342 cm^{-1} or 3343 cm^{-1} (O-H stretching in phenolic and aliphatic structures) as well as at 2935 cm^{-1} and 2970 cm^{-1} (C-H stretching of methyl, methylene) was more pronounced in the initial ex-KL compared to the s-KL. Also, well resolved spectrum was detected from ex-KL (Figure 5b) in the characteristic for lignins region from 1640 cm^{-1} (aromatic skeletal vibrations) to 1033 cm^{-1} (aromatic C-H deformation) and below.

The sulfur content has direct relation on stability and reactivity on lignin pyrolysis; the greater weight loss in lignosulfonate samples containing higher sulfite groups has been shown in publications. As the sulfur content decreases drastically in the pyrolyzed sample, especially for ex-KL (Figure 4b), the total amount of sulfur-containing compounds in the gas phase is higher from ex-KL pyrolysis by factor of 1.5 at high temperatures, and the residue becomes more stable, Figure 2. As a result, more residue yield is detected from pyrolysis of ex-KL at higher temperatures (47% at 700 ^{o}C, Figure 2) due to the expected less sulfur content which was also shown by XPS analysis of the char from ex-KL (sulfur atomic concentration, 0.74 %). On the other hand, high initial content of sulfur in s-KL (3.61% (w)), less release of sulfur-containing compounds into gas phase, high content of sulfur in residue (Sulfur atomic concentration = 3.95%) revealed to decreased yields of residue (40% at 700 ^{o}C) due to its instability at high temperatures.

Note that sulfur bonding in both lignins was not conclusively established based on FTIR analysis (Figure 5). The characteristic bonds containing sulfur are assigned mostly below 1400 cm^{-1} which are difficult to analyze due to the complex bands from various modes of vibration

(Abdelaziz & Hulteberg, 2017). The XPS analysis has qualitatively shown the existence of sulfur for initial lignins as well as corresponding chars; the surface atomic concentrations of elements are summarized in the e-supplementary data of this work.

It is also important to compare the chars from s-KL and ex-KL pyrolysis, respectively (Figure 5a: blue line) and (Figure 5b: black line). The FT-IR spectra of pyrolyzed Kraft lignins show that almost all the functional groups in both lignins have lower intensity due to thermal decomposition. More aromaticity (at 1442 cm^{-1}, aromatic skeletal vibration) has been seen for the char from pyrolysis of s-KL at concomitant appearance of surface carbonyl group at 1727 cm^{-1} (Figure 5a), while the char from ex-KL pyrolysis significantly stayed intact to the initial lignin structure.

The low yields and late release of tar compounds from s-KL pyrolysis (Figure 3b) may have direct relationship with the sulfur-containing compounds adsorbed or linked to the lignin macromolecule. Importantly, the maximal yields of tar compounds from s-KL pyrolysis (~ 300 ^{o}C, Figure 3b) match to the maximum yields of released sulfur-containing compounds at 300 ^{o}C-315 ^{o}C (Figure 4a) as well as with maximum rate of depolymerization of s-KL at ~ 300 ^{o}C, Figure 2. Therefore, the pretreatment of s-KL leading to less sulfur content in the initial ex-KL (2.91%) most probably favors early removal of sulfur compounds in the first stages of pyrolysis as well as accelerated pyrolysis of ex-KL and hence, release of large amounts of tar components.

3.3.1 Inhibitive effects of sulfur-containing compounds on depolymerization of KLs: A mechanistic explanation

Based on previous section results, the authors can assume that the depolymerization of KL samples, besides the pretreatment effect of the solvents, is activated at certain temperatures when the release of sulfur-containing compounds is effective. The early removal of sulfur from s-KL (and more effectively from ex-KL) pyrolysis at lower temperatures (175 ^{o}C-250 ^{o}C, Figure 4) can be attributed to the sulfur compounds adsorbed on the KL lattice (Dondi et al., 2014). It remains to be investigated whether these adsorbed sulfur-containing compounds affect the depolymerization rate of s-KL. This hypothesis is illustrated in Figure 6 via possible transformations of the one of the model compounds of lignin, para-coumaryl alcohol (p-CMA) to phenolic compounds by attacking of H atoms to the C_{α}=C_{β} double bond in case when the active reaction site is blocked by an adsorbed sulfur containing compound. Recently, our collaborators reported a comprehensive potential energy surface analysis of the p-CMA and p-CMA + H - atom systems using various DFT and *ab initio* protocols to examine the possible roles of the concerted molecular elimination and free-radical mechanisms in the formation of major products (Asatryan et al., 2017). The calculations particularly suggested a set of chemically-activated radical channels relevant to the low temperature product formation under pyrolysis conditions (Figure 6, upper two channels). The coordination (simple adsorption) of thiol-like compounds to the double bond moieties, Figure 6, may deactivate all processes involving the transformations of the side chains typical for lignin pyrolysis both at low as well as high temperatures (Asatryan et al., 2017).

Sulfur-containing compounds are well-known to play deactivating roles in heterogeneous catalysis (Argyle & Bartholomew, 2015). There is limited information on the suppressing/inhibiting effect of the sulfur-compounds on formation of such carcinogenic chemicals as dioxins, and the mechanism of suppression is unknown. Recent studies have indicated that the formation of metal sulfates coincides with PCDD/F inhibition (Fujimori T et al., 2014). A detailed understanding of the inhibition mechanism is beyond the scope of this work. The authors note only that our preliminary data supports the hypotheses provided in Feld-

Cook *et al.* (Feld-Cook EE et al., 2017) regarding the possible suppression resulting from the blocking of the active reactive centers by different agents such as sulfides, SO_2, or sulfur-containing organic compounds.

Therefore, the sulfur-containing compounds in KL constitute detrimental impurities and reducing the sulfur content in KL will favorably improve the yields of valuable products and chemicals. Lignins with a lower sulfur content could be a more useful feedstock to produce a variety of value-added products such as those reported in literature (Caballero et al., 1997; Evdokimov et al., 2018).

The sulfur-containing compounds, when released in gas phase, could dramatically change concentration of the active pool radicals such as H and OH (responsible for radical-chain depolymerization of lignin) as scavengers through reaction (1):

$$H\ (OH) + RSH \rightarrow RS\bullet + H_2\ (H_2O) \qquad (1)$$

The S-H bonds in alkane-thiols, CH_3SH and CH_3CH_2SH, are known to be weaker than the corresponding C–H bonds (87.5 and 87.6 kcal/mol versus *ca.* 94.2 kcal/mol, respectively) (Gunturu A., 2011). In the case of methyl thiol, it has been shown experimentally and theoretically that the dominant pathway for the reaction of H atoms with CH_3SH is the formation of methylthiyl radical (Kerr et al., 2015), reaction (1a):

$$H + CH_3SH \rightarrow CH_3S\bullet + H_2 \qquad (1a)$$

The authors note that the key role of the OH(H) radicals in pyrolysis of lignin and model compounds has been actively discussed in recent publications (Asatryan et al., 2017; Kawamoto, 2017; M. Akazawaa et al., 2015). Newly formed sulfur centered radicals RS• (reaction 1, chain "carrier change ") are more passive, and therefore exert a negative influence on the further depolymerization of KL. This could provide a rationale for the lower rates of the pyrolysis of KLs as the concentration of sulfur-containing compounds increases in the gas phase.

The thiyl radicals may also form from the dissociation of relatively weak persulfide –S-S-bond in intrinsic persulfides (R_2S_2) via reaction (2) (reported bond energy is less than 74 kcal/mol) (Vandeputte et al., 2010):

$$R_2S_2 \rightarrow 2\ RS\bullet \qquad (2)$$

Reaction 2 is one of the main initiation reactions of the decomposition of $(CH_3)_2S_2$ (formation of $RS_2\bullet$ is also considered in the gas phase (Vandeputte et al., 2010).

The activity of persulfides (R_2S_2) in the metabolism and mechanisms by which sulfur atoms are incorporated into biomolecules in biosynthetic reactions have been extensively discussed (Ollagnier-de-Choudens et al., 2003). Another possible source for the formation of thiyl radicals involving phenoxyl radicals (PhO•) (see Reaction 3 below) is the reactivity of PhO• radicals towards intracellular macromolecules (ascorbate, thiols, RSH, etc.) and membrane lipids which is more pronounced and have been discussed in literature. A thiyl radical (RS•) potentially can be generated in biological environments, (Stoyanovsky et al., 1995) as in reaction 3:

$$PhO\bullet + RSH \rightarrow PhOH + RS\bullet \qquad (3)$$

The formation of oxygen-centered phenoxy type PhO• radicals during lignin pyrolysis has been recently confirmed in a number of publications (Barekati-Goudarzi et al., 2017; Khachatryan et al., 2016; Kibet et al., 2012; Kim et al., 2014). A reaction pathway similar to that of reaction 3 could serve as an alternative route to remove more reactive PhO• radicals in process of lignin pyrolysis by replacing them with less active thiyl radicals, RS•. All afore-mentioned channels for the formation of thiyl radicals in the gas phase are sources likely to suppress the concentrations of OH(H) and PhO• pool radicals and hence, the rate of radical-chain decomposition pathways of lignin.

As regards the condensation reactions of sulfur-centered radicals, the authors note that whereas numerous reaction pathways for formation of thiyl radicals exist (reactions 1-3), no sulfur-containing biofuel compounds (likely to form during further reactions of thiyl radicals) were detected either in the present work or a recently published study (Han et al., 2018). Thus, the authors can infer that thiyl radicals are much more passive and that instead of insertion and addition reactions (to aromatic rings, unsaturated bonds etc. via the formation of sulfur-containing compounds), the self-condensation reaction of RS• (reaction 4) is dominant:

$$2CH_3S\bullet \rightarrow [(CH_3S\bullet)_2] \rightarrow CH_3\text{-}S\text{-}S\text{-}CH_3 \qquad (4)$$

Upon comparison with the reaction by participation of analogue $CH_3O\bullet$ radicals of reaction (5) with reaction (4);

$$2CH_3O\bullet \rightarrow [(CH_3O\bullet)_2] \rightarrow 2CH_2O + 2H \qquad (5)$$

one can see the highly significant advantage of self-condensation of $CH_3S\bullet$ over that of $CH_3O\bullet$ by comparing the corresponding rate constants of reactions 4 and 5 (NIST, 1998), with the ratio greater than 10, thus illustrating high dimerization capability of thiyl radicals:

$$k_4/k_5 = [4.0 \times 10^{-11}\ \text{cm}^3\text{/molecule.sec}] / [3.0 \times 10^{-12}\ \text{cm}^3\text{/molecule.sec}] > 10$$

Similarly, the rate constant of the addition reaction of $CH_3S\bullet$ to unsaturated hydrocarbons (e.g. ethylene) is in the order of 2.0×10^{-15} cm^3/molecule.sec, which is much slower than that for the self-condensation in reaction (4). Thus, these phenomena could explain the absence of sulfurized bio-oil products during pyrolysis of s-KL.

Nevertheless, abstraction or addition reactions by participation of sulfur-centered radicals may occur according to their rate constants, as evident in the formation of covalently linked S atoms in lignin macromolecule, for instance formation of thiirane, epo-sulfide bonds, 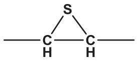

(addition of sulfur to unsaturated olefinic bond in the side chain of lignin) or organically bound sulfur thiol (-SH) (Evdokimov et al., 2018; Jiang et al., 2010). The authors note that the addition reactions of thiyl radicals to olefinic bonds depends on the environment of the double bond. For instance, the rate constants for addition of thiyl radical to propene is one order of magnitude higher (1.0×10^{-14} cm^3/molecule.sec) than that with ethene (2.0×10^{-15} cm^3/molecule.sec) when one hydrogen in ethene is replaced by methyl group-producing propene. These reactions while having minor occurrence in the gas phase cannot compete, however, with the condensation reactions of sulfur-centered radicals (reaction 4).

The addition reactions rate constants are much higher in case of free sulfur atom (S_0) – the rate constant of reaction 6 is significantly higher, in order of 10^{-12} cm^3/molecule.sec (NIST, 1998). This reaction may occur especially during the pulping process of black liquor. The authors note that during pulping processes, the ionic reactions are more preferable at elevated temperatures, 150 °C-170 °C (Li et al., 2011), leading to the formation of thiirane structure of the lignin:

$S + H_2C{=}CH\text{-}R \rightarrow H_2C\ (S)\ CH\text{-}R$ (like epoxide) (6)

The insertion reaction of elemental sulfur (ground state), an insertion phenomenon of sulfur into C-H bond (formation of organically bound sulfur (-SH)) with the rate constant in order of 10^{-14} cm^3/molecule.sec (Eberhard & Klaus, 1970), can be considered minor compared to the insertion into much weaker -C-S- bond in $(CH_3)_2S$ (or $(CH_3)_2S_2$), Reaction 7 ($k_7 = 3.43 \times 10^{-10}$ cm^3/molecule.sec) (Green et al., 1984):

$S + CH_3\text{-}S\text{-}CH_3 \rightarrow CH_3\text{-}S\text{-}S\text{-}CH_3$ (7)

Further insertion of S ether in C-S or –S-S- bonds in $(CH_3)_2S_2$ molecule can lead to the formation of CH_3-S-S-S-CH_3 detected in sulfur-products of pyrolysis of KL (Mu et al., 2013).

Finally, if the formation of sulfur-energized atoms in the gas phase during the pyrolysis of KL is assumed, then the dimerization termolecular reaction (8) by formation of S_2 can be one of the preferable pathways with high reaction rate constant, $k_8 = 1.18\ 10^{-29}\ cm^6/molecule^2.sec$ (NIST, 1998):

$$S + S + M \rightarrow S_2 + M \qquad (8)$$

Therefore, the absence of sulfurized bio-oil products during pyrolysis of s-KL is most likely, since the self-condensation reactions of S-centered radicals (including sulfur atoms) are dominant over addition/insertion/abstraction reactions towards the formation of bio-oil compounds.

3.3.2. Char formation

The high content of char produced from pyrolysis of KL, reaching up to 50 % or more (Brazil et al., 2018) is another interesting phenomenon to examine. The lowest residue content from pyrolysis of other types of lignins have been reported; for instance, char from hydrolytic lignin pyrolysis at high temperatures reaches up to 28-30 % (Barekati-Goudarzi et al., 2017), 26-33 % from Klason lignin (Yan et al., 2016), 18-25 % from Avicel lignin (Ranzi et al., 2017)????, etc.

In general, a reasonable explanation for the char formation from pyrolysis of lignin might be that the methide intermediate structures formed from the pyrolysis of lignin (or lignin model compounds) are easily polymerized via charring process (Asatryan et al., 2017). However, the methylation of phenolic hydroxyl groups, which suppresses the formation of methide structures, lowers the yield of the char (Kim et al., 2017). Similarly, the pretreatment of lignin phenolic hydroxyl, carboxyl and other functional groups by calcium hydroxide leads to less agglomeration during pyrolysis (Zhou et al., 2015).

Most probably, the mechanisms of charring processes are similar for all lignins including KL. However, KL differs from others because of its high content of sulfur as mentioned above (Evdokimov et al., 2018; Messmer et al., 2018) . Since sulfur-containing compounds suppress the free-radical fast oxidation reactions of KL macromolecules especially by lowering the concentration of OH/H, this phenomenon can be the main source of suspending further depolymerization of KLs and hence high content of unreacted lignin.

On the other hand, the radical - chain re-polymerization reactions can be also initiated by participation of, for instance, methylthiyl radicals $CH_3S\bullet$ formed in reaction 1. While the most favorable reaction of thiyl radicals is dimerization, as mentioned above, thiyl radicals to some extent can initiate re-polymerization reactions either in the gas phase or on the surface. This scenario may lead to new charring processes, while minor, among the schemes discussed for sulfur-free lignins (Asatryan et al., 2017).

Thus, since the sulfur-containing compounds deactivate the depolymerization processes and initial, non-pyrolyzed, and newly formed KL macromolecules (after re-polymerization) remain on the char, it follows that the residue content increases upon pyrolysis and that some amount of sulfur is also incorporated in the char content. This assertion on the amounts of sulfur detected in the char is corroborated in various publications (Beis et al., 2010; Zhang et al., 2012) as well as in the e-supplementary data of this work.

4. CONCLUSIONS

Fractional pyrolysis of two types of softwood Kraft lignin (s-KL) and extracted Kraft lignin (ex-KL) at 175 ^{o}C - 700 ^{o}C was investigated. Product analyses were performed on major groups observed – guaiacols, vanillin, phenolics, syringols, and sulfur-containing compounds.

The pretreatment of s-KL(sulfur content-3.61%) leads to less sulfur content in the initial ex-KL (2.91%) and favors early removal of sulfur compounds in the first stages of pyrolysis and release of large amounts of tar components. A mechanistic explanation of the inhibitive role of sulfur-compounds on bio-oil yields, products distribution, and high char content is presented.

ACKNOWLEDGEMENTS

This work was funded by the NSF EPSCoR program (OIA #1632854). The authors acknowledge a partial support from NSF grant (1805677) and the USDA-NIFA Hatch program. Published with the approval of the Director of the Louisiana Agricultural Experiment Station as manuscript #2019-232-33831**.** This study was also partially supported by Romania's "Competitiveness Operational Programme 2014-2020", Priority Axis 1: Research, Technological Development and Innovation (RD&I) to Support Economic Competitiveness and Business Development, Action 1.1.4. Attracting high-level personnel from abroad in order to enhance the RD capacity, ID/Cod My SMIS: P_37_768/schita: 103651; Contract No. 39/ 02.09.2016.

E-supplementary data of this work can be found in the online version of the paper.

Declarations of interest: none

REFERENCES

1. Abdelaziz, O.Y., Hulteberg, C.P. 2017. Physicochemical Characterisation of Technical Lignins for Their Potential Valorisation. *Waste and Biomass Valorization*, **8**(3), 859-869.

2. Argyle, M.D., Bartholomew, C.H. 2015. Heterogeneous Catalyst Deactivation and Regeneration: . *A Review. Catalysts.*, **5**(1), 145-269.
3. Asatryan, R., Bennadji, H., Bozzelli, J.W., Ruckenstein, E., Khachatryan, L. 2017. Molecular Products and Fundamentally Based Reaction Pathways in the Gas-Phase Pyrolysis of the Lignin Model Compound p-Coumaryl Alcohol. *Journal of Physical Chemistry A*, **121**(18), 3352-3371.
4. Barekati-Goudarzi, M., Boldor, D., Marculescu, C., Khachatryan, L. 2017. Peculiarities of Pyrolysis of Hydrolytic Lignin in Dispersed Gas Phase and in Solid State. *Energy & Fuels*, **31**(11), 12156-12167.
5. Beis, S., Mukkamala, S., Hill, N., Joseph, J., Baker, C., Jensen, B., Stemmler, E., Wheeler, C., Frederick, B., Van Heiningen, A. 2010. Fast pyrolysis of lignins. *BioResources*, **5**(3), 1408-1424.
6. Bennadji, H., Khachatryan, L., Lomnicki, S.M. 2018. Kinetic modeling of cellulose fractional pyrolysis. *Energy & Fuels*, **32**(3), 3436-3446.
7. Brazil, T.R., Costa, R.N., Massi, M., Rezende, M.C. 2018. Structural, morphological, and thermal characterization of kraft lignin and its charcoals obtained at different heating rates. *Materials Research Express*, **5**(4), 045502.
8. Brebu, M., Cazacu, G., Chirila, O. 2011. Pyrolysis of lignin—a potential method for obtaining chemicals and/or fuels. *Cellulose Chemistry and Technology*, **45**(1), 43.
9. Brodin, I., Sjöholm, E., Gellerstedt, G. 2010. The behavior of kraft lignin during thermal treatment. *Journal of Analytical and Applied Pyrolysis*, **87**(1), 70-77.
10. Brodin, I., Sjöholm, E., Gellerstedt, G. 2009. *Kraft lignin as feedstock for chemical products: The effects of membrane filtration*.
11. Caballero, J., Font, R., Marcilla, A. 1997. Pyrolysis of Kraft lignin: yields and correlations. *Journal of Analytical and Applied Pyrolysis*, **39**(2), 161-183.
12. Dondi, D., Zeffiro, A., Speltini, A., Tomasi, C., Vadivel, D., Buttafava, A. 2014. The role of inorganic sulfur compounds in the pyrolysis of Kraft lignin. *Journal of Analytical and Applied Pyrolysis*, **107**, 53-58.
13. Eberhard, L., Klaus, G. 1970. Direct Photolysis of Carbonyl Sulfide in Solution. Reactions of Singlet D Sulfur Atoms in the Liquid Phase. *Journal of the American Chemical Society* **92**(8), 2221-2227.
14. Evdokimov, A.N., Kurzin, A.V., Fedorova, O.V., Lukanin, P.V., Kazakov, V.G., Trifonova, A.D. 2018. Desulfurization of kraft lignin. *Wood Science and Technology*, 1-10.
15. Feld-Cook EE, Bovenkamp-Langlois L, SM., L. 2017. Effect of Particulate Matter Mineral Composition on Environmentally Persistent Free Radical (EPFR) Formation. . *Environ Sci Technol.*, **51**(18), 10396-10402.
16. Fujimori T, Nishimoto Y, Shiota K, M., T. 2014. Contrasting effects of sulfur dioxide on cupric oxide and chloride during thermochemical formation of chlorinated aromatics. *Environ Sci Technol.* , **48**(23).
17. Green, M., Lown, E., Strausz, O.P. 1984. Reactions of S atoms with dimethyl sulfide and thietane. *Journal of the American Chemical Society*, **106**(23), 6938-6946.
18. Gunturu A., A.J., Bozzelli, J. W. 2011. Thermochemistry, bond energies and internal rotor barriers of methyl sulfinic acid, methyl sulfinic acid ester and their radicals. *Journal of Physical Organic Chemistry*, **24**(5), 366-377.

19. Han, T., Sophonrat, N., Evangelopoulos, P., Persson, H., Yang, W., Jönsson, P. 2018. Evolution of sulfur during fast pyrolysis of sulfonated Kraft lignin. *Journal of Analytical and Applied Pyrolysis*, **133**, 162-168.
20. Islam, M.N., Taki, G., Rana, M., Park, J.-H. 2018. Yield of phenolic monomers from lignin hydrothermolysis in subcritical water system. *Industrial & Engineering Chemistry Research*, **57**(14), 4779-4784.
21. Jiang, G., Nowakowski, D.J., Bridgwater, A.V. 2010. A systematic study of the kinetics of lignin pyrolysis. *Thermochimica Acta*, **498**(1-2), 61-66.
22. Karnjanakom, S., Guan, G., Asep, B., Du, X., Hao, X., Yang, J., Samart, C., Abudula, A. 2015. A green method to increase yield and quality of bio-oil: ultrasonic pretreatment of biomass and catalytic upgrading of bio-oil over metal (Cu, Fe and/or Zn)/γ-Al 2 O 3. *RSC Advances*, **5**(101), 83494-83503.
23. Kawamoto, H. 2017. Lignin pyrolysis reactions. *Journal of Wood Science*, **63**(2), 117.
24. Kerr, K.E., Alecu, I.M., Thompson, K.M., Gao, Y.D., Marshall, P. 2015. Experimental and Computational Studies of the Kinetics of the Reaction of Atomic Hydrogen with Methanethiol. *Journal of Physical Chemistry A*, **119**(28), 7352-7360.
25. Khachatryan, L., Xu, M.-x., Wu, A.-j., Pechagin, M., Asatryan, R. 2016. Radicals and molecular products from the gas-phase pyrolysis of lignin model compounds. Cinnamyl alcohol. *Journal of analytical and applied pyrolysis*, **121**, 75-83.
26. Kibet, J., Khachatryan, L., Dellinger, B. 2012. Molecular products and radicals from pyrolysis of lignin. *Environmental science & technology*, **46**(23), 12994-13001.
27. Kim, K.H., Bai, X., Brown, R.C. 2014. Pyrolysis mechanisms of methoxy substituted α-O-4 lignin dimeric model compounds and detection of free radicals using electron paramagnetic resonance analysis. *Journal of Analytical and Applied Pyrolysis*, **110**, 254-263.
28. Kim, K.H., Dutta, T., Walter, E.D., Isern, N.G., Cort, J.R., Simmons, B.A., Singh, S. 2017. Chemoselective Methylation of Phenolic Hydroxyl Group Prevents Quinone Methide Formation and Repolymerization During Lignin Depolymerization. *ACS Sustainable Chemistry & Engineering*, **5**(5), 3913-3919.
29. Kouisni, L., Gagné, A., Maki, K., Holt-Hindle, P., Paleologou, M. 2016. LignoForce system for the recovery of lignin from black liquor: feedstock options, odor profile, and product characterization. *ACS Sustainable Chemistry & Engineering*, **4**(10), 5152-5159.
30. Li, W., Sun, N., Stoner, B., Jiang, X., Lu, X., Rogers, R.D. 2011. Rapid dissolution of lignocellulosic biomass in ionic liquids using temperatures above the glass transition of lignin. *Green Chemistry*, **13**(8), 2038-2047.
31. Løhre, C., Halleraker, H.V., Barth, T. 2017. Composition of Lignin-to-Liquid Solvolysis Oils from Lignin Extracted in a Semi-Continuous Organosolv Process. *International journal of molecular sciences*, **18**(1), 225.
32. M. Akazawaa, Y. Kojimab, Y. Kato. 2015. Pyrolysate formation from four different phenyl propanols and classification of the initial reaction pathways, 4 (2015) *International Journal of Renewable Energy Technology Research*, **4**(3), 1-14.
33. McCarthy, J.L., Islam, A. 1999. Lignin Chemistry, Technology, and Utilization: A Brief History. in: *Lignin: Historical, Biological, and Materials Perspectives*, Vol. 742, American Chemical Society, pp. 2-99.
34. Melro, E., Alves, L., Antunes, F., Medronho, B. 2018. A brief overview on lignin dissolution. *Journal of Molecular Liquids*.

35. Messmer, N.R., Guerrini, L.M., Oliveira, M.P. 2018. Effect of unmodified kraft lignin concentration on the emulsion and miniemulsion copolymerization of styrene with n-butyl acrylate and methacrylic acid to produce polymer hybrid latex. *Polymers for Advanced Technologies*, **29**(3), 1094-1106.
36. Mu, W., Ben, H., Ragauskas, A., Deng, Y. 2013. Lignin pyrolysis components and upgrading—technology review. *BioEnergy Research*, **6**(4), 1183-1204.
37. NIST. 1998. Chemical Kinetics Database 17 G. *Gaithersburg*, MD.
38. Norgren, M., Edlund, H. 2001. Stabilisation of kraft lignin solutions by surfactant additions. *Colloids and Surfaces A: Physicochemical and Engineering Aspects*, **194**(1-3), 239-248.
39. Nowakowski, D.J., Bridgwater, A.V., Elliott, D.C., Meier, D., de Wild, P. 2010. Lignin fast pyrolysis: results from an international collaboration. *Journal of Analytical and Applied Pyrolysis*, **88**(1), 53-72.
40. Ollagnier-de-Choudens, S., Lascoux, D., Loiseau, L., Barras, F., Forest, E., Fontecave, M. 2003. Mechanistic studies of the SufS–SufE cysteine desulfurase: evidence for sulfur transfer from SufS to SufE. *FEBS letters*, **555**(2), 263-267.
41. Ranzi, E., Debiagi, P.E.A., Frassoldati, A. 2017. Mathematical Modeling of Fast Biomass Pyrolysis and Bio-Oil Formation. Note II: Secondary Gas-Phase Reactions and Bio-Oil Formation. *ACS Sustainable Chemistry & Engineering*, **5**(4), 2882-2896.
42. Stoyanovsky, D.A., Goldman, R., Claycamp, H.G., Kagan, V.E. 1995. Phenoxyl Radical-Induced Thiol-Dependent Generation of Reactive Oxygen Species: Implications for Benzene Toxicity. *Archives of Biochemistry and Biophysics*, **317**(2), 315-323.
43. Svensson, S. 2008. Minimizing the sulphur content in Kraft lignin.
44. Vandeputte, A.G., Reyniers, M.F., Marin, G.B. 2010. Theoretical Study of the Thermal Decomposition of Dimethyl Disulfide. *Journal of Physical Chemistry A*, **114**(39), 10531-10549.
45. Vishtal, A.G., Kraslawski, A. 2011. Challenges in industrial applications of technical lignins. *BioResources*, **6**(3), 3547-3568.
46. Waters, C.L., Janupala, R.R., Mallinson, R.G., Lobban, L.L. 2017. Staged thermal fractionation for segregation of lignin and cellulose pyrolysis products: An experimental study of residence time and temperature effects. *Journal of analytical and applied pyrolysis*, **126**, 380-389.
47. Yan, K., Liu, F., Chen, Q., Ke, M., Huang, X., Hu, W., Zhou, B., Zhang, X., Yu, H. 2016. Pyrolysis characteristics and kinetics of lignin derived from enzymatic hydrolysis residue of bamboo pretreated with white-rot fungus. *Biotechnology for biofuels*, **9**(1), 76.
48. Yang, H., Yan, R., Chen, H., Lee, D.H., Zheng, C. 2007. Characteristics of hemicellulose, cellulose and lignin pyrolysis. *Fuel*, **86**(12-13), 1781-1788.
49. Zhang, M., Resende, F.L., Moutsoglou, A., Raynie, D.E. 2012. Pyrolysis of lignin extracted from prairie cordgrass, aspen, and Kraft lignin by Py-GC/MS and TGA/FTIR. *Journal of Analytical and Applied Pyrolysis*, **98**, 65-71.
50. Zhou, S., Brown, R.C., Bai, X. 2015. The use of calcium hydroxide pretreatment to overcome agglomeration of technical lignin during fast pyrolysis. *Green Chemistry*, **17**(10), 4748-4759.

List of Figures

Figure 1. Schematic diagram of the STDS (system for thermal diagnostic studies) for pyrolysis of biomass (lignin, cellulose etc.).

Figure 2. Thermal decomposition profiles and their first order derivatives (dashed lines) of softwood Kraft lignin (s-KL) and extracted Kraft lignin (ex-KL); the samples were not dried before pyrolysis.

Figure 3. (a) The yields of grouped guaiacol and guaiacol derivatives (guaiacol; 6-methyl guaiacol; 4-ethyl guaiacol) from fractional pyrolysis of s-KL (blue solid line) and ex-KL (brown solid line). The dashed lines are cumulative yields of guaiacol derivatives calculated from experimental data for both lignins. **(b)** The yields of total tar (guaiacols + vanillin + phenolics+ syringols) from fractional pyrolysis of s-KL (blue solid line) and ex-KL (brown solid line). The dashed lines are cumulative yields of the tar calculated from experimental data for both lignins.

Figure 4. (a) Peak intensities of sulfur-containing compounds (dimethyl sulfide, dimethyl disulfide, methane thiol, sulfur dioxide) obtained as a function of temperature from the fractional pyrolysis of s-KL and ex-KL. **(b)** Cumulative average yields of sulfur-containing compounds (dimethyl sulfide, dimethyl disulfide, methane thiol, sulfur dioxide) from pyrolysis of s-KL (blue dashed line) and ex-KL (brown dashed line) (NOTE: the temperature scales are not identical since the bar graphs do not have all temperatures that are displayed on the cumulative chart).

Figure 5. (a) FT-IR spectra of initial (red) and pyrolyzed (blue) softwood Kraft lignin fractions. **(b)**: FT-IR spectra of initial (green) and pyrolyzed (black) extracted Kraft lignin fractions.

Figure 6. Thiol hypothetic adsorption on reaction active center (double C_{α}=C_{β} bond) of side chain propenol units may deactivate further transformation one of lignin model compounds, para-coumaryl alcohol by attacking of H atoms from the radical pool(Asatryan et al., 2017).

Declaration of interests

☒ The authors declare that they have no known competing financial interests or personal relationships that could have appeared to influence the work reported in this paper.

☐The authors declare the following financial interests/personal relationships which may be considered as potential competing interests:

HIGHLIGHTS

- Fractional pyrolysis of softwood Kraft lignin (s-KL) and methanol-extracted (ex-KL) biomass at 175 °C - 700 °C is investigated.
- Sulfur contaminants inhibit depolymerization of Kraft lignin during fractional pyrolysis.
- Sulfur contaminants has dramatic effects on the production of bio-oil compounds.
- Mechanistic explanations of the inhibitive role of sulfur contaminations on depolymerization of both lignins are presented.

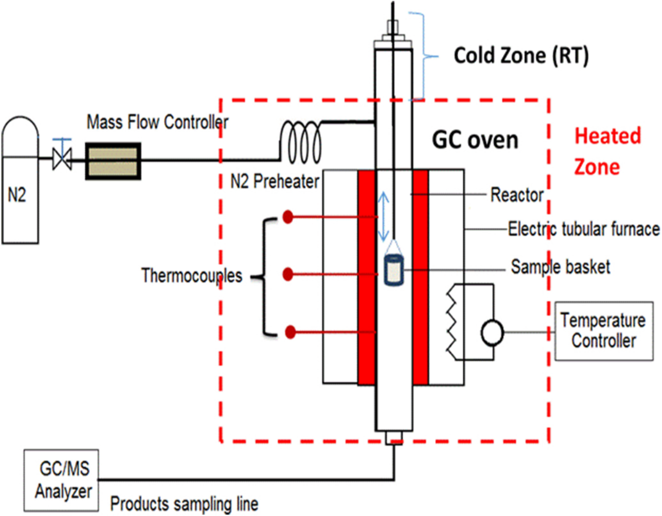
Cold Zone (RT)
Mass Flow Controller
GC oven
Heated Zone
N2
N2 Preheater
Reactor
Electric tubular furnace
Thermocouples
Sample basket
Temperature Controller
GC/MS Analyzer
Products sampling line

Figure 1

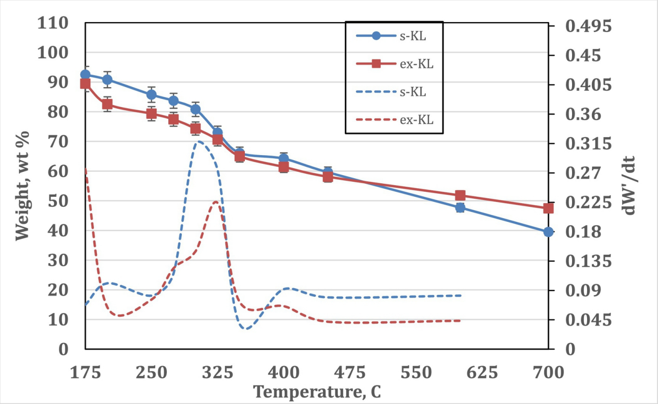
Weight, wt %
110
100
90
80
70
60
50
40
30
20
10
0
175
250
325
400
475
550
625
700
Temperature, C
0.495
0.45
0.405
0.36
0.315
0.27
0.225
0.18
0.135
0.09
0.045
0
dW'/dt
s-KL
ex-KL
s-KL
ex-KL

Figure 2

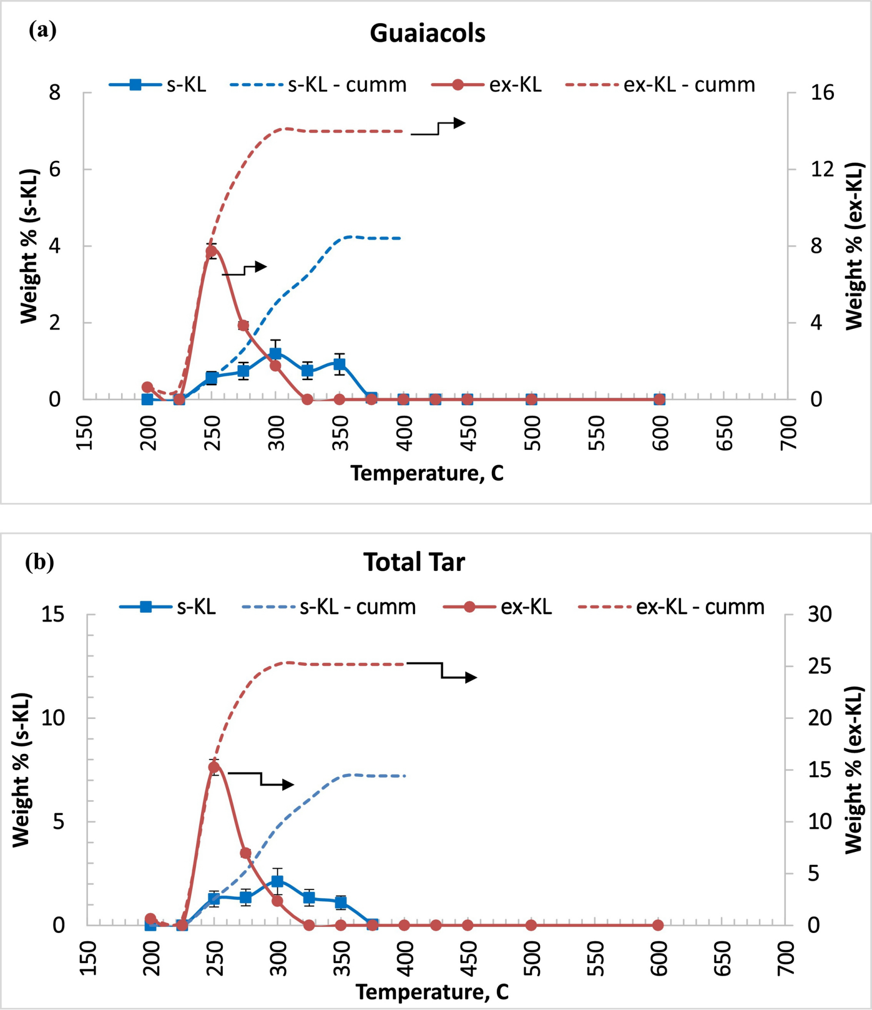
(a)
Guaiacols
s-KL
s-KL - cumm
ex-KL
ex-KL - cumm
Weight % (s-KL)
0
2
4
6
8
Weight % (ex-KL)
0
4
8
12
16
Temperature, C
150
200
250
300
350
400
450
500
550
600
650
700
(b)
Total Tar
s-KL
s-KL - cumm
ex-KL
ex-KL - cumm
Weight % (s-KL)
0
5
10
15
Weight % (ex-KL)
0
5
10
15
20
25
30
Temperature, C
150
200
250
300
350
400
450
500
550
600
650
700

Figure 3

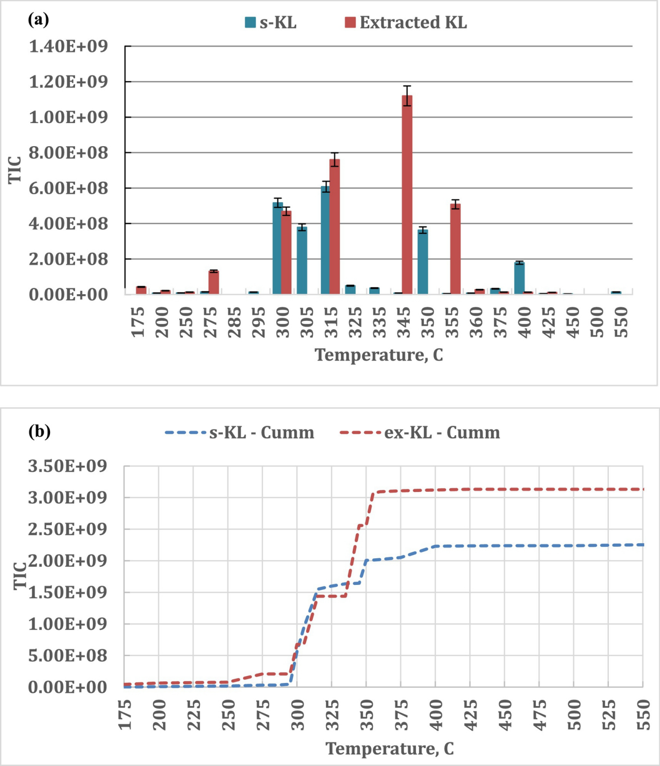
(a)
s-KL
Extracted KL
TIC
1.40E+09
1.20E+09
1.00E+09
8.00E+08
6.00E+08
4.00E+08
2.00E+08
0.00E+00
175
200
250
275
285
295
300
305
315
325
335
345
350
355
360
375
400
425
450
500
550
Temperature, C
(b)
s-KL - Cumm
ex-KL - Cumm
TIC
3.50E+09
3.00E+09
2.50E+09
2.00E+09
1.50E+09
1.00E+09
5.00E+08
0.00E+00
175
200
225
250
275
300
325
350
375
400
425
450
475
500
525
550
Temperature, C

Figure 4

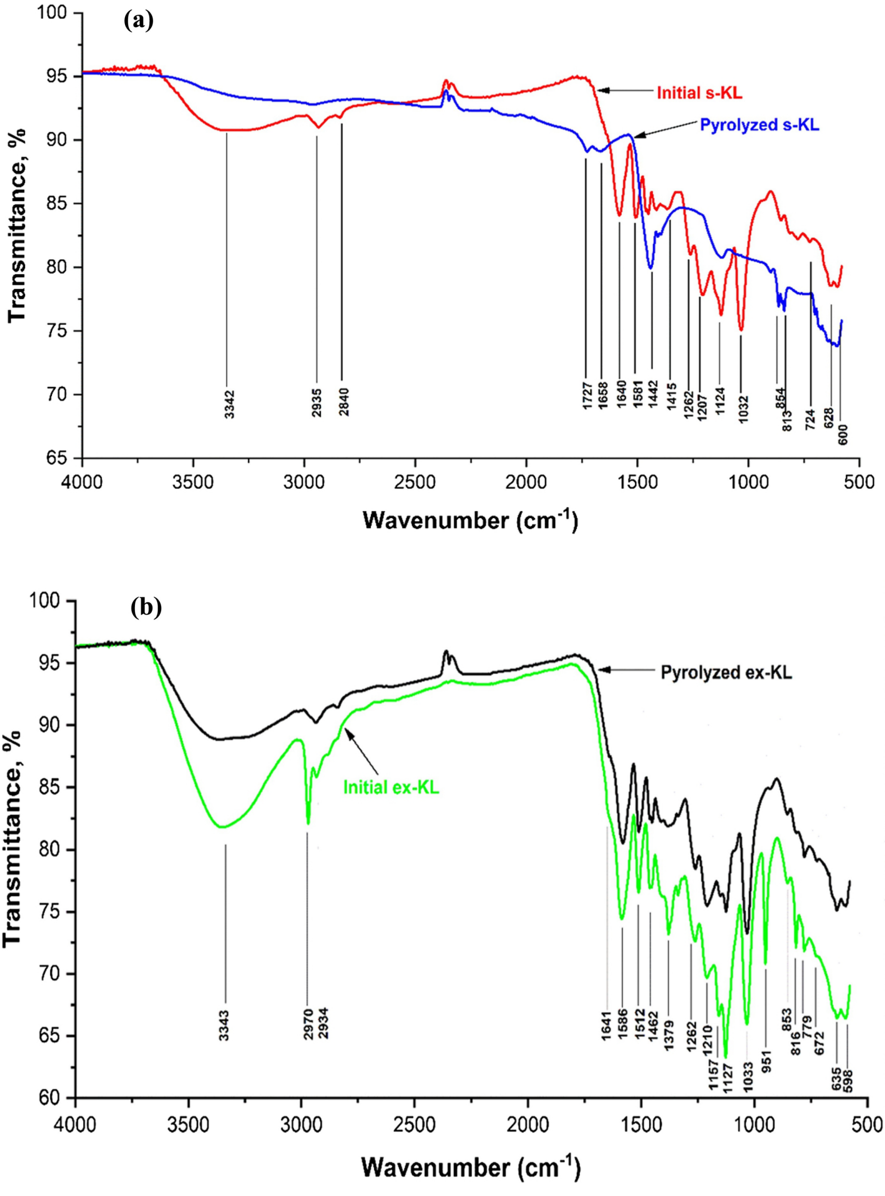
(a)
Transmittance, %
100
95
90
85
80
75
70
65
Wavenumber (cm-1)
4000
3500
3000
2500
2000
1500
1000
500
Initial s-KL
Pyrolyzed s-KL
3342
2935
2840
1727
1658
1640
1581
1442
1415
1262
1207
1124
1032
854
813
724
628
600
(b)
Transmittance, %
100
95
90
85
80
75
70
65
60
Wavenumber (cm-1)
4000
3500
3000
2500
2000
1500
1000
500
Pyrolyzed ex-KL
Initial ex-KL
3343
2970
2934
1641
1586
1512
1462
1379
1262
1210
1157
1127
1033
951
853
816
779
672
635
598

Figure 5

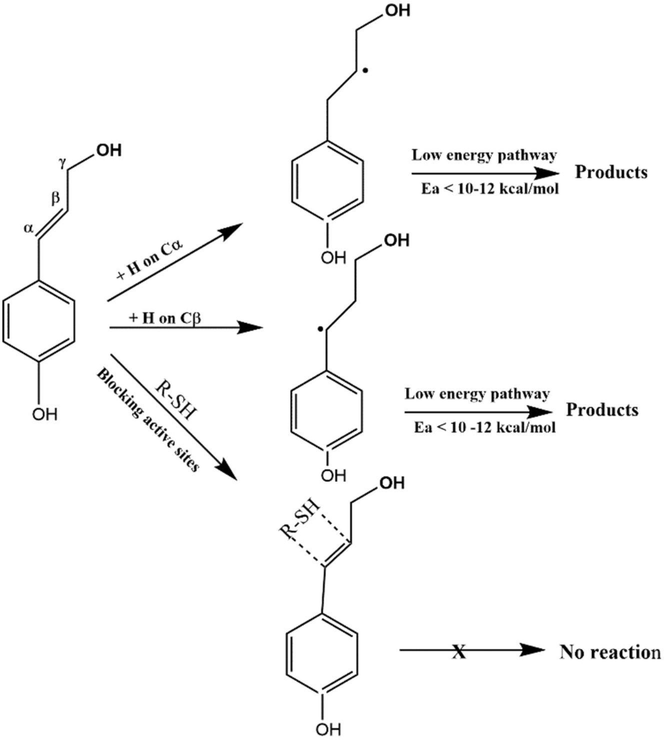
OH
γ
β
α
OH
+ H on Cα
+ H on Cβ
R-SH
Blocking active sites
OH
OH
Low energy pathway
Ea < 10-12 kcal/mol
Products
OH
OH
Low energy pathway
Ea < 10 -12 kcal/mol
Products
OH
R-SH
OH
X
No reaction

Figure 6